Electrocatalytic oxidation of ethanol on Pt, Pt-Ru and Pt-Sn nanoparticles in polymer electrolyte membrane fuel cell—Role of oxygen permeation

Andrzej Jablonski, Adam Lewera *

Department of Chemistry, University of Warsaw, ul. Pasteura 1, 02-093 Warsaw, Poland

ABSTRACT

We have recently shown that in low temperature, polymer-electrolyte membrane direct ethanol fuel cells oxygen permeating from cathode is able to chemically oxidize ethanol at the anode surface [A. Jablonski, P.J. Kulesza, A. Lewera, Journal of Power Sources 196 (2011) 4714–4718]. Such process is responsible for significant amounts of acetaldehyde and acetic acid present at anode outlet, which are not related to the flow of electric current in external circuit. Here, for the first time, we report unbiased distribution of products of ethanol electrooxidation on Pt, Pt-Ru and Pt-Sn as a function of fuel cell voltage (under load) and temperature. We show here that for Pt anode and for cell voltage above 300 mV oxidation of ethanol to acetic acid does not occur as a result of electric current flow, but it is caused exclusively by chemical reaction between ethanol and oxygen permeating from cathode. This explains the obvious contradiction, which can be found in scientific literature regarding ethanol electrooxidation on Pt. Namely acetic acid is not observed in spectroelectrochemical, *ex situ* experiments in conditions comparable to working direct ethanol fuel cell, where it is detected in case of *in situ*, fuel cell experiments.

Relation between unbiased distribution of products and anode catalyst's type, cell voltage, cell discharge current and temperature is also discussed. Oxygen permeation via Nafion 117 at 80 °C expressed in unit of electric current has been estimated to be at least 2.5–3.5 mA/cm^2.

© 2011 Elsevier B.V. All rights reserved.

1. Introduction

Polymer electrolyte membrane fuel cells (PEMFCs) have attracted significant attention as potential alternative power sources due to their high theoretical efficiency in converting chemical to electric energy. Direct ethanol PEM fuel cells (DEFCs) are utilizing ethanol as a fuel, which has many advantages, i.e. high energy density, ease of production and handling, low toxicity and environmental compatibility [1,2]. Platinum-based anodes, especially carbon-supported Pt, Pt-Sn and Pt-Ru, are commonly used in DEFCs due to the highest current densities, which can be obtained [1–10].

For better understanding of ethanol oxidation reaction (EOR) on Pt-based materials, a broad range of techniques were used to analyze possible reaction paths and their final- and by-products. For that purpose most frequently spectroscopic [9–14], chromatographic [9,15] and differential electrochemical mass spectrometry (DEMS) were used [13,14,16–18]. From that research EOR is known to occur via many paths of complex sequential reactions and potential-induced equilibria and, despite the significant work devoted to its understanding, many aspects of EOR are still unclear

[13,19,20]. Overall, oxidation of ethanol on Pt-based materials leads mainly to CO_2, CO, acetaldehyde and acetic acid [15,21,22]. Acetaldehyde and acetic acid are main products of incomplete (respectively 2- or 4-electrons per ethanol molecule) oxidation, as compared to 12 electrons, which can be obtained per ethanol molecule when CO_2 is the final product. Additionally, acetic acid is a dead-end for EOR, when occurring in DEFC, as it cannot be further oxidized in the potential range typical for a working fuel cell [11,12].

While the selectivity is compared between different materials, pure Pt is known for is ability to break carbon—carbon bond to the highest degree as compared to any known bi-metallic catalysts, and only relatively new ternary systems containing Rh can be compared to pure Pt in that aspect [23,24]. The main drawback of using pure Pt as anode catalyst for EOR is the fact, that it is easily poisoned by CO, which results in lower current densities obtained, as compared to bi-metallic systems containing Pt [3,4]. For instance Pt-Ru and Pt-Sn are characterized by higher current densities, but at the same time they produce relatively more acetaldehyde and acetic acid and less CO_2, as compared to pure Pt [7,9,15,25]. Thus the analysis of selectivity towards CO_2, acetaldehyde and acetic acid, beside the polarization curves and other commonly used measurements, is a valuable source of information, which allows better characterization and understanding of anode materials [15,26,27].

* Corresponding author. Tel.: +48 22 822 0211x524; fax: +48 22 822 0211.
E-mail address: alewera@chem.uw.edu.pl (A. Lewera).

Analysis of products of EOR reaction, occurring at anode in working fuel cell, is a complementary technique to the above-mentioned spectroscopic and DEMS methods due to the fact that, for instance, it does not provide information about catalyst's surface poisons. However it allows to comment on the fuel cell as a whole, i.e. to analyze the influence of parasitic processes occurring in fuel cell, which cannot be addressed in *ex situ* experiments. For instance, it is well known, that the polymer membranes (i.e. Nafion) are prone to permeation of components present in anodic and cathodic compartments, causing so-called "mixed potential" phenomenon. It occurs when, for instance, fuel molecules are present in the cathode compartment due to permeation from anode side. This subsequently causes unwanted redox reactions and poisoning of cathode, which drives the cathode potential down [28–38].

Permeation of fuel from anode to cathode side is relatively well studied, but to our best knowledge no other groups are studying the oxygen permeation process in relation to fuel cells. We have recently shown [39], that oxygen, permeating from cathode to anode side in a working DEFC, is able to oxidize ethanol, and such parasitic process obviously is not connected to electric current flowing in the external circuit [39]. This severely influences distribution of ethanol oxidation products when DEFC is tested under load and, as we will show below, can explain the discrepancy between the results obtained for *in situ* and *ex situ* experiments. For the first time, we report here the systematic and unbiased EOR product distribution for three most common anode catalysts used in DEFC, as a function of temperature and cell potential and correlate them to previous experiments and spectroscopic, *ex situ* literature data.

2. Experimental

All chemicals were of analytical grade and were used without further purification. MiliQ (18 MΩ) water was used in preparation of all ethanol solutions. High purity (N5.2) gases from Air Products were used to deaerate ethanol solutions (Ar) and as a cathode gas (O_2). The flow of oxygen was maintained at 15 scm^3 s^{-1} using a mass flow controller from Sierra Instruments and the backpressure of 200 kPa (29 psi) was kept. 5% Nafion solution from Sigma–Aldrich and DuPont Nafion N117 membrane were used to prepare the membrane-electrode assemblies. Dry, carbon-supported Pt, Pt-Ru (1:1) and Pt-Sn (3:1) nanoparticles containing 20% of metal deposited on Vulcan XC-72 carbon, manufactured by ETEK (BASF) were used as anode (Pt, Pt-Ru or Pt-Sn) and cathode (Pt) catalysts. The catalyst's suspensions in solution of Nafion in ethanol/water (1:1) mixture were prepared, where relation of Nafion to catalysts' amounts were kept constant to obtain 32 wt.% of Nafion in dry catalytic layer. The suspension was mixed for at least 1 h and subsequently painted on carbon paper support to obtain anode and cathode metal loading of 1.0 mg cm^{-2}. After painting, the carbon paper supported electrodes were hot pressed using ca. 830 kPa (120 psi) at 120 °C for 5 min.

Fuel cell hardware from Fuel Cell Technologies Inc. was used. It consisted of two graphite plates with single serpentine flow pattern and 10 cm^2 active area. Cell voltage and current were controlled using EG&G Princeton Applied Research 362 Scanning Potentiostat. As a rule: (i) when tested under load the fuel cell voltage was not allowed to drop below 300 mV; (ii) following the fuel cell voltage/current change, the system was stabilized for at least 30 min before starting the product analysis; (iii) after fuel cell temperature change, the system was stabilized for at least 2 h. Fuel was fed using a peristaltic pump at 1.56 cm^3 min^{-1} rate. Based on preliminary experiments the concentration of ethanol in water was optimized and 0.2 mol dm^{-3} proved to be the optimum for qualitative and quantitative analysis of products of ethanol electrooxidation in
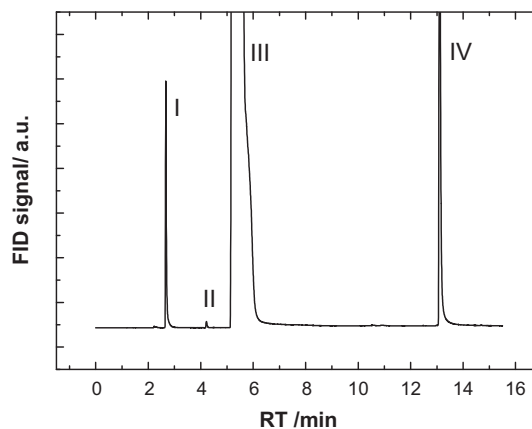

Fig. 1. Gas chromatogram of a mixture leaving PEMFC. Anode: 1 mg/cm^2 of Pt-Sn (20% on XC-72), 80 °C, N117 as a membrane. Current density 15 mA/cm^2. Peaks at 2.9 (I), 4.5 (II), 5.5 (III), and 13.3 (IV) min are (I): acetaldehyde, (II): ethyl acetate, (III): ethanol and (IV): acetic acid, respectively.

PEMFC using gas chromatography (see below). Ethanol solution was constantly deaerated (using Ar gas), prior and during introduction to the anode compartment of the fuel cell, to avoid the possible oxidation of ethanol (or acetaldehyde) at anode catalyst's surface by oxygen dissolved from air.

Mixture containing products of ethanol oxidation was sampled from the port directly at the anode outlet, then introduced to Hewlett Packard 5890 Series II gas chromatograph (GC), which allowed for separation and qualitative and quantitative determination of the components of the mixture leaving fuel cell. For qualitative determination a Hewlett Packard 5971A mass selective detector (MSD) was used, where for quantitative analysis a flame ionization detector (FID) was used. FID signal was calibrated for acetaldehyde and acetic acid in 0–5 mol% range using ethanol as internal standard [40].

3. Results and discussion

The use of GC with MS and FI detectors is fast, very precise, and practically on-line technique, which allowed us to investigate the distribution of products of ethanol oxidation in low temperature fuel cell in broad range of conditions. An example analysis of the mixture leaving working fuel cell anode (Pt-Sn) at typical conditions (15 mA/cm^2, 80 °C) confirms that, except ethanol, acetaldehyde, acetic acid and ethyl acetate can be separated and identified using GC/MS and FID (Fig. 1). This observation is in good agreement with data published previously [11,12,14,15,17–19,21,22,26,27,32,41]. Presence of ethyl acetate is obviously a result of esterification, which decreases the amount of acetic acid detected. To avoid the possible underestimation of acetic acid amounts, in the following studies, we adjusted the amount of acetic acid detected by the amount of ethyl acetate at 1:1 molar ratio. Overall the registered amount of ethyl acetate was not significant, i.e. at 0.05% level.

The results of analysis of EOR products in DEFC, as a function of cell voltage and temperature, for Pt anode, are shown in Fig. 2A. It is worth to note that even at open circuit conditions (OC, when cell current equals to zero), the registered amounts of acetic acid and acetaldehyde are significant for all three temperatures (Fig. 2A, points at the highest cell voltage for each temperature). Obviously those products cannot be related to catalytic electrooxidation of ethanol, and we attribute them to the parasitic process, where ethanol is chemically oxidized on Pt surface by oxygen permeating from cathode, as we shown previously [39].
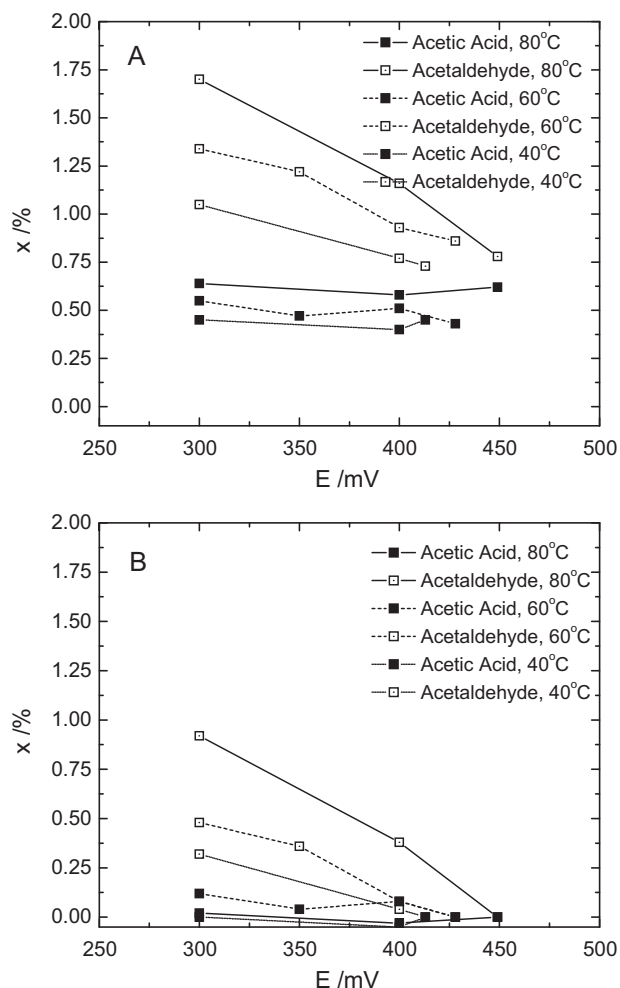
Fig. 2. Products of ethanol electrooxidation versus cell voltage in case of direct ethanol fuel cell, where Pt anode has been used. Part A shows raw data, part B shows data after correction for oxygen crossover.

To obtain reliable results regarding the correlation between electric current flow and the acetaldehyde and acetic acid produced the above mentioned parasitic process of ethanol oxidation by oxygen permeating from cathode compartment must be corrected for. It is known, that the gas permeation through Nafion membrane is dependent on temperature, pressure, humidity and concentration [29,30], but to our knowledge there are no reports that this process is dependent on cell voltage. Based on that, we assume that the rate of oxygen permeation should be approximately constant at given cell temperature, regardless of cell voltage, and the data under load were corrected for the oxygen permeation by simply subtracting the amount of products detected at OC. Data for Pt anode, corrected for oxygen permeation are shown in Fig. 2B.

After the correction it become clear, that ethanol cannot be electrochemically oxidized to acetic acid on Pt and when cell voltage is equal or higher than 300 mV. There are many reports, when acetic acid was detected and attributed to ethanol electrooxidation on Pt anode in DEFC, even at relatively high cell voltages, but the effect of oxygen permeation was never accounted for [7,15,27,32]. Based on our results we postulate, that in case of direct ethanol fuel cells with Pt anode and Nafion membranes acetic acid is produced mainly as a result of chemical oxidation by oxygen permeating from cathode, providing that the cell voltage is equal or higher than 300 mV. This is in agreement with spectroscopic data, where no adsorbed acetate groups are detected on Pt surface at similar conditions. Namely Wieckowski and co-workers [12] used broad band sum-frequency

generation (BB-SFG) technique to study the ethanol oxidation on Pt surface in absence of oxygen, and found that up to 600 mV vs. RHE, the Pt surface is occupied by CO and no acetate group can be detected. When potential was increased above 600 mV, the CO was oxidized and the acetate groups could be detected. To compare those data to our results we assume that the cathode has a potential of ca. 800 mV vs. RHE, which is a typical potential at which the oxygen reduction reaction on platinum occurs. As a result electrode potential of 600 mV and more, as in the above mentioned BB-SFG studies [12], equals to cell voltage of 200 mV and below. Concluding, from the BB-SFG data [12] it can be expected that acetic acid can be produced as a result of electrooxidation of ethanol on Pt only when cell voltage is equal or lower than 200 mV, which is in good agreement with our results. From the impedance analysis of EOR on Pt performed by Lasia and co-workers [42] the same conclusion about CO adsorption on Pt as a function of electrode potential, and its inhibiting role on electrooxidation of ethanol to acetic acid can be drawn. Recently also Heinen and co-workers addressed the problem of ethanol, acetaldehyde and acetic acid adsorption on polycrystalline Pt, using ATR-FTIRS, and found a similar relationship between electrode potential, presence of CO and electrooxidation of ethanol to acetic acid (which is detected in form of adsorbed acetate groups) [11]. In particular adsorbed acetate groups were detected when anode potential was cycled towards positive values, with onset at ca. 0.7 V and maximum at about 1.0 V vs. RHE. This observation correlates with decrease of the signal for linearly bonded CO, and authors suggests, that CO-free surface is a prerequisite for presence of acetic acid [11]. Only after adsorbed CO is stripped (oxidized) from Pt surface at high electrode potential (low cell voltage) the electrooxidation of ethanol to acetic acid can occur. For instance Behm and co-workers observed acetic acid in *ex situ* experiments when Pt/C electrode has been cycled in 0.1 M ethanol in 0.5 H_2SO_4 in a wide potential range [22].

From all the results above it is clear that electrooxidation of ethanol to acetic acid is strongly correlated to the adsorption of CO on Pt, and cannot commence as long as Pt surface is covered with it. CO can be oxidized (stripped) at electrode potentials higher than 600 mV, which corresponds to cell voltages lower than 200 mV. Our studies, when correction for oxygen permeation is applied, are in good agreement with those results and can explain the observed discrepancy between the *ex situ*, spectroscopic data and analysis of products of EOR on Pt anode in working DEFC.

Knowing that ethanol can be electrooxidized to acetaldehyde in the whole cell voltage range (Fig. 2B), another possible source of acetic acid can be identified, which is electrooxidation of acetaldehyde to acetic acid. But this process must be excluded in working DEFC, as it is known that the electrochemical oxidation of acetaldehyde to acetic acid is characterized by two voltammetric peaks, occurring at potential of ca. 0.9 V (with a shoulder at the lower potential side) and 1.3 V [18]. Corresponding anode potentials cannot be obtained in working direct ethanol fuel cell and such reaction must be excluded as a potential source of acetic acid at fuel cell conditions.

In case of Pt-Ru anode, both acetaldehyde and acetic acid were detected, even after correction for oxygen crossover (see Fig. 3A and B for raw and corrected for oxygen permeation data). It is worth to note that, in case of Pt-Ru, the parasitic ethanol oxidation reaction does not significantly change the relative amounts of acetaldehyde and acetic acid, as it did in case of pure platinum.

Presence of acetic acid in case of Pt-Ru can be explained based on the known properties of this material in EOR. Namely ruthenium in Pt-Ru alloys is able to activate water and provide specific chemical groups (mainly OH) necessary to oxidize the poisoning species adsorbed on platinum surface. This is a well known phenomenon called "bi-functional" (or chemical) mechanism, first described by Watanabe and Motoo for methanol electrooxidation on Pt-Ru [43].
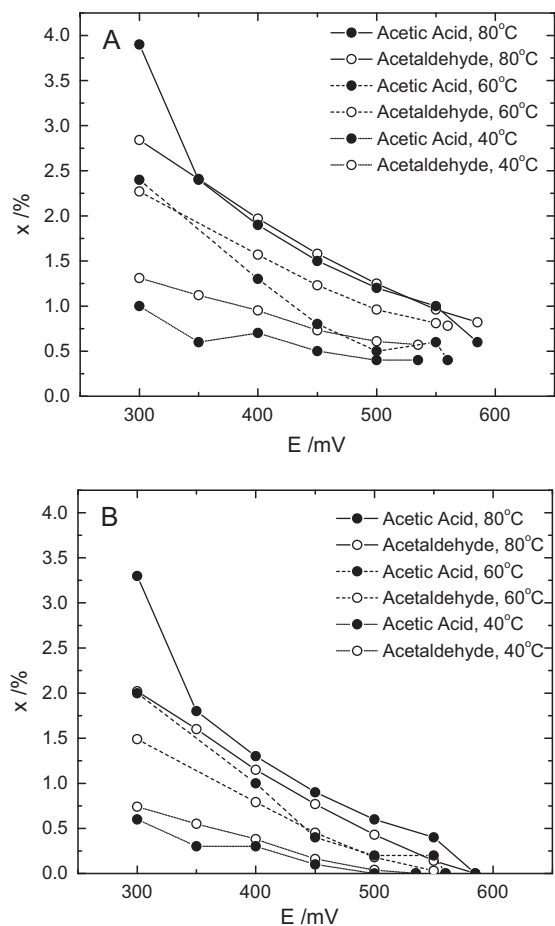
Fig. 3. Products of ethanol electrooxidation versus cell voltage in case of direct ethanol fuel cell, where Pt-Ru anode has been used. Part A shows raw data, part B shows data after correction for oxygen crossover.

Fig. 4. Products of ethanol electrooxidation versus cell voltage in case of direct ethanol fuel cell, where Pt-Sn anode has been used. Part A shows raw data, part B shows data after correction for oxygen crossover.

It is also known that addition of Ru to Pt lowers the strength of CO adsorption on Pt-Ru in comparison to pure Pt, most probably due to change in electronic properties of the surface [44–46] which results in oxidation of CO on Pt-Ru at lower potential than on Pt, with onset at ca. 400–450 mV vs. RHE in case of Pt-Ru alloys with composition close to 1:1 [47]. Those properties of Pt-Ru most probably allow for electrooxidation of ethanol to acetic acid at its surface at much lower potential. This can be observed as non-zero acetic acid amounts registered for the whole cell voltage range (Fig. 3B). Also the increase in acetic acid amount, when cell voltage drops to 300 mV (Fig. 5B), can be explained based on correlations between adsorbed CO and presence of acetic acid, as discussed above for Pt [11,12]. Namely at that potential CO oxidation commences on Pt-Ru [47], which frees even more surface sites, preoccupied with CO, required for electrooxidation of ethanol to acetic acid, which is observed as increase in acetic acid amount registered at fuel cell anode outlet (Fig. 5B).

Regarding the temperature and cell voltage dependence on distribution of products of EOR on Pt-Ru, it can be observed that in the 40–80 °C temperature range, the molar ratio of acetaldehyde to acetic acid is close to 1:1 (see Figs. 3 and 5B). The amount of acetic acid increases from ca. 40% to 60%, when cell temperature increases from 40 °C to 80 °C (Fig. 5B). In relation to literature data it is worth to note, that Wang et al. observed similar amounts, namely that acetic acid accounts for ca. 70% of the DEFC products in similar conditions [48]. Tsiakaras and co-workers observed that the amount of acetaldehyde varies from 45 to 70% depending on discharge current and temperature but the dependence between the
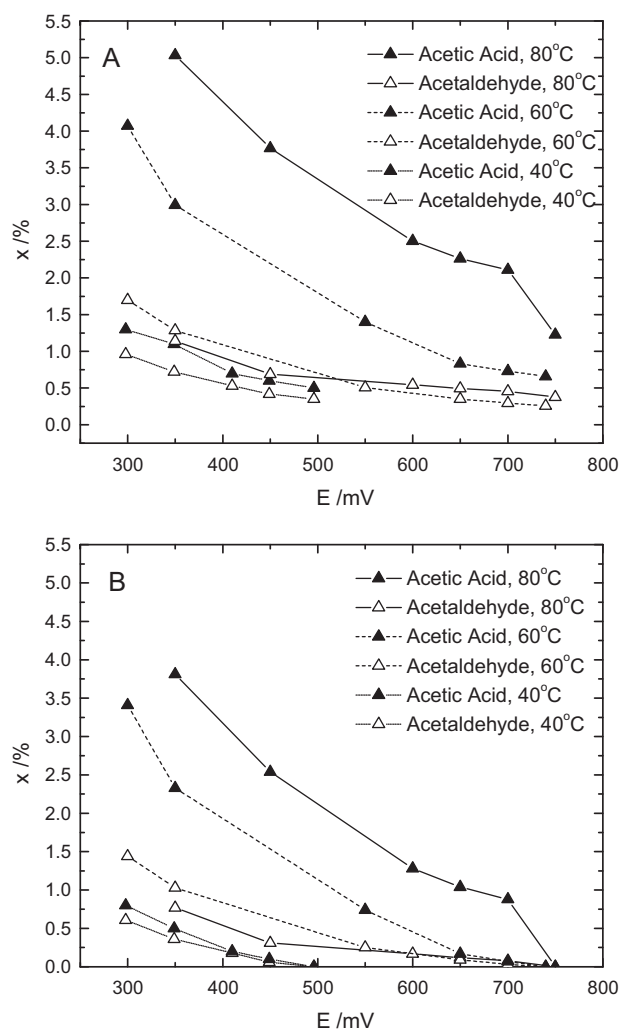
temperature and products for a given cell voltage has not been presented [26]. In general our data follow the trend already observed, and the differences in absolute amounts can be attributed to the fact, that our data are corrected for effects of oxygen permeation, which has not been done before.

In case of Pt-Sn, the amount of acetic acid is significantly higher as compared to Pt-Ru (see Fig. 4A and B and compare Fig. 5A and B). Namely the acetic acid accounts for at least 60% of products at 40 °C, and ca. 90% at 80 °C. The presence of acetic acid can be attributed to the same mechanism, based on oxidation of CO at lower potentials, as in case of Pt-Ru. No significant difference of products distribution has been found as a function of fuel cell voltage, regardless of temperature (see Fig. 5A).

Overall the reported concentration of acetic acid and acetaldehyde produced when ethanol is oxidized on Pt-Sn varies in literature, due to the fact that it is dependent on many factors, such as catalyst's morphology, cell voltage and discharge current, temperature and ethanol concentration [10,18,21,22,26,27,49]. But the overall trend, that electrooxidation of ethanol on Pt-Sn results in more acetic acid than on Pt-Ru (Figs. 5 and 6) has been always observed, when those two catalysts are compared in similar conditions [48,50]. Namely Li and Pickup [50] have observed, that in case of Pt-Sn in the cell voltage range between 356 and 402 mV, acetic acid has accounted for between 94 and 98% of all products,
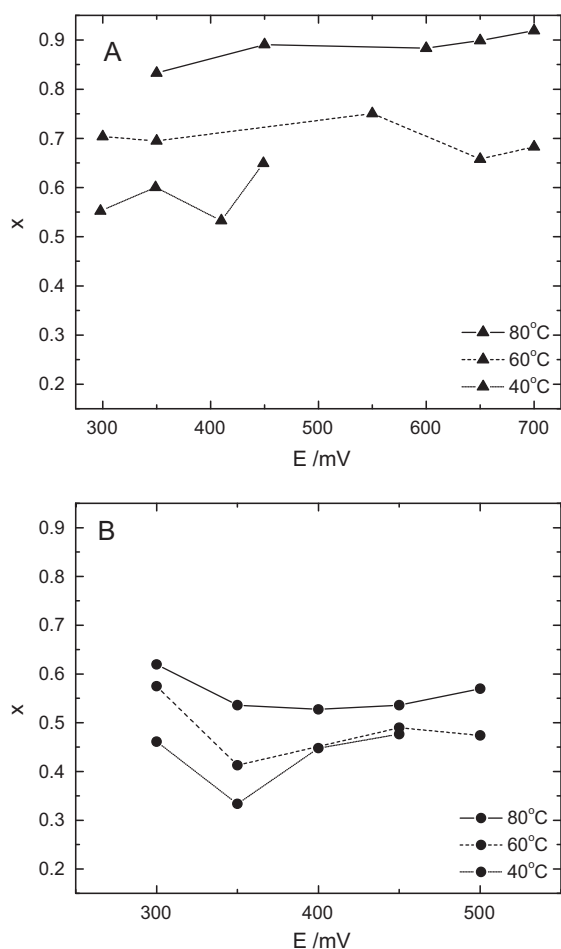
Fig. 5. Relative amount of acetic acid, versus cell voltage. Part A is for Pt-Sn anode, part B for Pt-Ru anode. In case of Pt anode acetaldehyde is the only product of electrooxidation of ethanol.

where in case of Pt-Ru acetic acid was on 77% level at 281 mV. Wang et al. reported from 90 to 94% of acetic acid for Pt-Sn and from 73 to 80% in case of Pt-Ru [48]. Also, when only one type of catalysts is investigated, the similar results are obtained. For instance Leger and co-workers observed acetic acid concentration between 75 and 80% for Pt-Sn at 80 °C [15]. Our data agree with those observations,
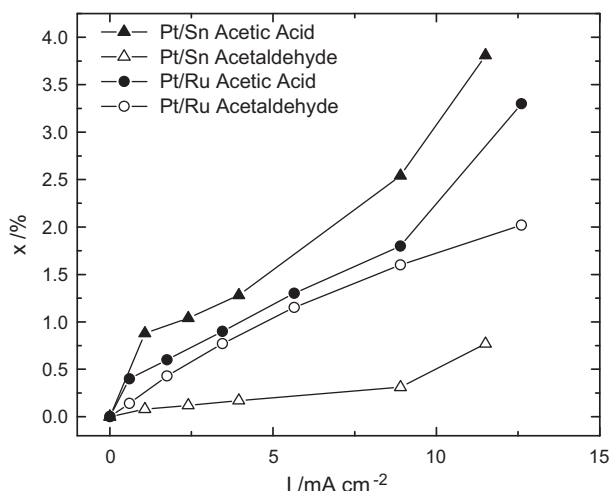

Fig. 6. Amount of acetic acid and acetaldehyde as a function of current density.

but provide more precise values, due to the applied correction for oxygen crossover.

Using the concentration data collected for Pt-Sn we estimated the current associated with oxygen permeation for Nafion 117 membrane as a function of pressure. For this estimation we used acetaldehyde and acetic acid concentration data collected at DEFC anode outlet at OC conditions at different oxygen pressure. It increases from 2.63 mA for zero to 3.46 mA for 210 kPa oxygen backpressure. It is worth to note that the values obtained are lower estimates, as chemical oxidation of ethanol at the surface of catalyst is at least in part limited by activity of the catalyst itself [39], and it cannot be excluded that some of the unreacted oxygen is still present in the anode outlet stream.

It is interesting to note that, for both catalysts, when current density increases, the relative amount of acetic acid does not change significantly (Figs. 5 and 6), which suggests that both paths of ethanol oxidation, leading to acetaldehyde and acetic acid occurs at approximately the same relative rate. The main difference between the Pt-Ru and Pt-Sn is the ratio between the acetaldehyde and acetic acid (Fig. 6). It can be attributed to the fact, that Pt-Sn is known to activate water and provide the OH groups to higher degree than Pt-Ru. Another conclusion which can be drawn is that those systems are very similar in terms of CO_2 production, as in both cases, for any given discharge current and observed product distribution, the charge is balanced by the different concentration of acetic acid and acetaldehyde (Fig. 6). Increased electrocatalytic activity, in terms of higher registered currents which can be obtained from DEFC with Pt-Ru anode as compared to DEFC with Pt anode can be attributed to more effective (4 electrons) oxidation of ethanol to acetic acid on this material, but the significant drawback is that the CO_2 production significantly decreases in Pt-Ru [7,9,15,25]. Further increase in activity of Pt-Sn, as compared to Pt-Ru anodes in DEFC can be attributed to the higher degree of ethanol electrooxidation to acetic acid on Pt-Sn. On Pt-Sn acetic acid accounts for over than 90% at 80 °C, as compared do ca. 70% for Pt-Ru at the same temperature.

Slight (ca. 5%) further improvement in registered currents could be obtained for Pt-Sn anodes, if acetic acid would be the only product. It is worth to note here, that increase of the cell current due to higher acetic acid yield only is generally not a promising way, as it is known, that acetic acid cannot be further oxidized at the conditions of the working fuel cell, which effectively makes it a dead-end of this reaction [19]. As a result the whole EOR process when acetic acid is the final product, will result in only 1/3rd of the amount of energy, which could be theoretically obtained per given volume of ethanol.

To obtain any significantly higher DEFC currents, as currently obtained on Pt-Sn, the new materials must be developed. Such new, potential catalyst must be characterized by higher turnover frequency, the ability to scission the C–C bond to higher degree and resistance to CO poisoning. This, as well as previous studies emphasize the need for new catalysts, applicable to electrooxidation of ethanol at low temperature.

4. Conclusions

We have demonstrated that, in direct ethanol fuel cell the oxygen permeation process is responsible for the parasitic, chemical oxidation of ethanol to acetic acid and acetaldehyde. This process significantly changes the distribution of products at the anode outlet, especially in case of Pt anode, where only acetaldehyde is observed as a product of electrocatalytical oxidation of ethanol, for cell voltages above 300 mV and temperature in the 40–80 °C range. Parasitic oxidation of ethanol to acetaldehyde and acetic acid, occurring in the working fuel cell is responsible for the discrepancy present in the scientific literature, regarding production

of acetic acid at Pt anode in direct ethanol fuel cells and ex situ experiments, where ethanol electrooxidation on Pt surface is investigated.

The data corrected for oxygen permeation show that the observed difference in activity between Pt-Ru and Pt-Sn can be attributed to the higher yield of acetic acid on Pt-Sn in the investigated range of cell voltages and discharge currents. As the acetic acid is a dead end of the electrooxidation of ethanol in the fuel cell conditions, this questions the applicability of Pt-Sn to real life systems.

Acknowledgment

References

[1] C. Lamy, E.M. Belgsir, J.M. Leger, Journal of Applied Electrochemistry 31 (2001) 799–809.
[2] C. Lamy, A. Lima, V. LeRhun, F. Delime, C. Coutanceau, J.M. Leger, Journal of Power Sources 105 (2002) 283–296.
[3] W.J. Zhou, Z.H. Zhou, S.Q. Song, W.Z. Li, G.Q. Sun, P. Tsiakaras, Q. Xin, Applied Catalysis B: Environmental 46 (2003) 273–285.
[4] W.J. Zhou, B. Zhou, W.Z. Li, Z.H. Zhou, S.Q. Song, G.Q. Sun, Q. Xin, S. Douvartzides, A. Goula, P. Tsiakaras, Journal of Power Sources 126 (2004) 16–22.
[5] W.J. Zhou, S.Q. Song, W.Z. Li, G.Q. Sun, Q. Xin, S. Kontou, K. Poulianitis, P. Tsiakaras, Solid State Ionics 175 (2004) 797–803.
[6] W.J. Zhou, W.Z. Li, S.Q. Song, Z.H. Zhou, L.H. Jiang, G.Q. Sun, Q. Xin, K. Poulianitis, S. Kontou, P. Tsiakaras, Journal of Power Sources 131 (2004) 217–223.
[7] F. Vigier, S. Rousseau, C. Coutanceau, J.M. Leger, C. Lamy, Topics in Catalysis 40 (2006) 111–121.
[8] P.E. Tsiakaras, Journal of Power Sources 171 (2007) 107–112.
[9] S.Q. Song, W.J. Zhou, Z.H. Zhou, L.H. Jiang, G.Q. Sun, Q. Xin, V. Leontidis, S. Kontou, P. Tsiakaras, International Journal of Hydrogen Energy 30 (2005) 995–1001.
[10] J.M. Leger, S. Rousseau, C. Coutanceau, F. Hahn, C. Lamy, Electrochimica Acta 50 (2005) 5118–5125.
[11] M. Heinen, Z. Jusys, R.J. Behm, Journal of Physical Chemistry C 114 (2010) 9850–9864.
[12] R.B. Kutz, B. Braunschweig, P. Mukherjee, R.L. Behrens, D.D. Dlott, A. Wieckowski, Journal of Catalysis 278 (2011) 181–188.
[13] T. Iwasita, E. Pastor, Electrochimica Acta 39 (1994) 531–537.
[14] B. Bittins-Cattaneo, S. Wilhelm, E. Cattaneo, H.W. Buschmann, W. Vielstich, Berichte Der Bunsen-Gesellschaft: Physical Chemistry Chemical Physics 92 (1988) 1210–1218.
[15] S. Rousseau, C. Coutanceau, C. Lamy, J.M. Leger, Journal of Power Sources 158 (2006) 18–24.
[16] A.A. Abd-El-Latif, E. Mostafa, S. Huxter, G. Attard, H. Baltruschat, Electrochimica Acta 55 (2010) 7951–7960.
[17] J.P.I. de Souza, S.L. Queiroz, K. Bergamaski, E.R. Gonzalez, F.C. Nart, Journal of Physical Chemistry B 106 (2002) 9825–9830.
[18] H. Wang, Z. Jusys, R.J. Behm, Journal of Power Sources 154 (2006) 351–359.
[19] H. Hitmi, E.M. Belgsir, J.M. Leger, C. Lamy, R.O. Lezna, Electrochimica Acta 39 (1994) 407–415.
[20] F.C. Simoes, D.M. dos Anjos, F. Vigier, J.M. Leger, F. Hahn, C. Coutanceau, E.R. Gonzalez, G. Tremiliosi, A.R. de Andrade, P. Olivi, K.B. Kokoh, Journal of Power Sources 167 (2007) 1–10.
[21] F. Vigier, C. Coutanceau, F. Hahn, E.M. Belgsir, C. Lamy, Journal of Electroanalytical Chemistry 563 (2004) 81–89.
[22] H. Wang, Z. Jusys, R.J. Behm, Journal of Physical Chemistry B 108 (2004) 19413–19424.
[23] A. Kowal, M. Li, M. Shao, K. Sasaki, M.B. Vukmirovic, J. Zhang, N.S. Marinkovic, P. Liu, A.I. Frenkel, R.R. Adzic, Nature Materials 8 (2009) 325–330.
[24] M. Li, A. Kowal, K. Sasaki, N. Marinkovic, D. Su, E. Korach, P. Liu, R.R. Adzic, Electrochimica Acta 55 (2010) 4331–4338.
[25] H. Wang, Z. Jusys, R.J. Behm, Journal of Applied Electrochemistry 36 (2006) 1187–1198.
[26] G. Andreadis, V. Stergiopoulos, S. Song, P. Tsiakaras, Applied Catalysis B: Environmental 100 (2010) 157–164.
[27] D.D. James, D.V. Bennett, G.C. Li, A. Ghumman, R.J. Helleur, P.G. Pickup, Electrochemistry Communications 11 (2009) 1877–1880.
[28] N.W. Deluca, Y.A. Elabd, Journal of Polymer Science, Part B: Polymer Physics 44 (2006) 2201–2225.
[29] M. Inaba, T. Kinumoto, M. Kiriake, R. Umebayashi, A. Tasaka, Z. Ogumi, Electrochimica Acta 51 (2006) 5746–5753.
[30] S.S. Kocha, J.D. Yang, J.S. Yi, AIChE Journal 52 (2006) 1916–1925.
[31] V. Neburchilov, J. Martin, H. Wang, J. Zhang, Journal of Power Sources 169 (2007) 221–238.
[32] D.D. James, P.G. Pickup, Electrochimica Acta 55 (2010) 3824–3829.
[33] P.E. Tsiakaras, G.M. Andreadis, A.K.M. Podias, Journal of Power Sources 181 (2008) 214–227.
[34] P. Tsiakaras, G. Andreadis, Chemical Engineering Science 61 (2006) 7497–7508.
[35] C. Eickes, P. Piela, J. Davey, P. Zelenay, Journal of the Electrochemical Society 153 (2006) A171–A178.
[36] V.S. Silva, J. Schirmer, R. Reissner, B. Ruffmann, H. Silva, A. Mendes, L.M. Madeira, S.P. Nunes, Journal of Power Sources 140 (2005) 41–49.
[37] U. Krewer, K. Sundmacher, Journal of Power Sources 154 (2006) 153–170.
[38] K. Scott, A.K. Shukla, C.L. Jackson, W.R.A. Meuleman, Journal of Power Sources 126 (2004) 67–75.
[39] A. Jablonski, P.J. Kulesza, A. Lewera, Journal of Power Sources 196 (2011) 4714–4718.
[40] S.V. Cherepitsa, S.M. Bychkov, A.N. Kovalenko, A.L. Mazanik, N.M. Selemina, O.B. Seredinskaya, Journal of Analytical Chemistry 58 (2003) 368–371.
[41] K. Taneda, T. Taniyama, Y. Yamazaki, Electrochemistry 72 (2004) 700–702.
[42] M.-L. Tremblay, D. Guay, A. Lasia, 9th International Microsymposium on Electrochemical Impedance Analysis, Rovinj, Croatia, June, 2011.
[43] M. Watanabe, S. Motoo, Journal of Electroanalytical Chemistry 60 (1975) 267–273.
[44] M.T.M. Koper, T.E. Shubina, R.A. van Santen, Journal of Physical Chemistry B 106 (2002) 686–692.
[45] T.E. Shubina, M.T.M. Koper, Electrochimica Acta 47 (2002) 3621–3628.
[46] F.B. de Mongeot, M. Scherer, B. Gleich, E. Kopatzki, R.J. Behm, Surface Science 411 (1998) 249–262.
[47] H.A. Gasteiger, N. Markovic, P.N. Ross, E.J. Cairns, Journal of Physical Chemistry 98 (1994) 617–625.
[48] Q. Wang, G.Q. Sun, L. Cao, L.H. Jiang, G.X. Wang, S.L. Wang, S.H. Yang, Q. Xin, Journal of Power Sources 177 (2008) 142–147.
[49] M.J. Giz, G.A. Camara, Journal of Electroanalytical Chemistry 625 (2009) 117–122.
[50] G.C. Li, P.G. Pickup, Journal of Power Sources 161 (2006) 256–263.